Direct mapping of ^{19}F in ^{19}FDG-6P in brain tissue at subcellular resolution using soft X-ray fluorescence

2013 J. Phys.: Conf. Ser. 463 012003

(http://iopscience.iop.org/1742-6596/463/1/012003)

Direct mapping of ^{19}F in ^{19}FDG-6P in brain tissue at subcellular resolution using soft X-ray fluorescence

C Poitry-Yamate[1,4], A Gianoncelli[2], G Kourousias[2], B Kaulich[3], M Lepore[1,4], R Gruetter[1,4,5] and **M Kiskinova[2]**

[1]Biomedical Imaging Center, Ecole Polytechnique Fédérale de Lausanne, Switzerland
[2]ELETTRA – Sincrotrone Trieste S.C.p.A., Trieste, Italy
[3]Diamond Light Source Ltd, Harwell Science and Innovation Campus, Oxfordshire, UK
[4]Radiology Department, University of Lausanne, Switzerland
[5]Radiology Department, University of Geneva, Switzerland

E-mail:carole.poitry-yamate@epfl.ch

Abstract. Low energy x-ray fluorescence (LEXRF) detection was optimized for imaging cerebral glucose metabolism by mapping the fluorine LEXRF signal of ^{19}F in ^{19}FDG, trapped as intracellular ^{19}F-deoxyglucose-6-phosphate (^{19}FDG-6P) at 1µm spatial resolution from 3µm thick brain slices. ^{19}FDG metabolism was evaluated in brain structures closely resembling the general cerebral cytoarchitecture following formalin fixation of brain slices and their inclusion in an epon matrix. 2-dimensional distribution maps of ^{19}FDG-6P were placed in a cytoarchitectural and morphological context by simultaneous LEXRF mapping of N and O, and scanning transmission x-ray (STXM) imaging. A disproportionately high uptake and metabolism of glucose was found in neuropil relative to intracellular domains of the cell body of hypothalamic neurons, showing directly that neurons, like glial cells, also metabolize glucose. As ^{19}F-deoxyglucose-6P is structurally identical to ^{18}F-deoxyglucose-6P, LEXRF of subcellular ^{19}F provides a link to *in vivo* ^{18}FDG PET, forming a novel basis for understanding the physiological mechanisms underlying the ^{18}FDG PET image, and the contribution of neurons and glia to the PET signal.

1. Introduction

Among the biological and medical applications combining low energy (soft) x-ray fluorescence (LEXRF) and scanning transmission x-ray microscopy (STXM) [**1**], brain energy metabolism has not been addressed. It is well established that glucose, the brain's principle energy fuel substrate, is essential to maintaining mature brain function; however, its cell-specificity has not yet been completely established. This is regrettable since this issue is key to understanding the mechanism of the tripartite synapse, i.e. presynaptic and postsynaptic neurons and glial processes, quantitating the physiological mechanisms underlying positron emission tomography (PET) images [**2**], and assessing the contribution of neurons and glia to the PET signal.

^{18}FDG (Fluoro-Deoxy-D-glucose) PET is the gold standard in the non-invasive imaging and quantitative evaluation of brain glucose metabolism, both in clinical and research settings. Use of the glucose analogue Deoxy-D-glucose (DG) isolates DG transport into the cell through specific glucose transporter proteins and its intracellular phosphorylation to 2-deoxy-D-glucose-6-phosphate (DG-6P), subsequently trapped in the metabolically active cell in proportion to the rate of glycolysis and at concentrations that can reach µmol/g, detectable by NMR [**3**].

In the present study we have used the structurally identical PET glucose analogue, albeit nonradiolabeled, i.e., ^{19}F-fluoro-deoxy-D-glucose (^{19}FDG) to map ^{19}F in ^{19}FDG-6P at subcellular resolution.

Synchrotron-based X-ray fluorescence imaging is based on secondary (fluorescent) photon emission, unique for each element of the periodic table irradiated with a high flux of photons with sufficient energy that results in the removal of an element's core level electrons. The XRF spectrum therefore contains information on the abundance of a specific elemental constituent in the specimen. Using an X-ray microprobe and scanning the specimen allows 2-dimensional mapping of the sample's elemental distribution at submicron spatial resolution [1]. Since the cross-section of fluorescence emission -- a process based on the photoelectric effect -- depends on the primary photon energy for light elements, such as C, O, N, F etc, sufficient signal can be obtained using soft X-rays. Using low energy XRF (LEXRF), the fluorescent emission of ^{19}F, monitored at 676 eV, is directly related to the cellular compartment where DG-6P is trapped in the brain cell.

We recently demonstrated the feasibility of direct mapping of cerebral glucose metabolism *in situ* at subcellular resolution using LEXRF detection of ^{19}FDG-6P by reproducing the expected localization and gradients of glucose metabolism in glial cells from mammalian retina and periventricular hypothalamus [**4**]. Here, the LEXRF measurements were extended to brain structures more closely resembling the general cerebral cytoarchitecture, following the upgrade of the Twinmic instrument with 4 more fluorescence detectors; introducing endogenous low Z elemental mapping, combined with absorption and phase contrast images, further extended the identification of morphological and structural landmarks and features of the preparation.

2. Methods

2.1 Metabolic ^{19}FDG experiments

The hypothalamus was rapidly excised from brains of rats, decapitated under pentobarbital (65mg/kg) anesthesia. Brain slices ≤ 300μm in thickness were prepared and transferred to glucose (10mM) containing-bicarbonate-buffered Ringer's solution (BBRS, 37^{O}C, pH, 7.4). After 6o min slices were washed of D-glucose and then superfused for 50 min with a mixture of 4 mM ^{19}FDG and 1mM D-glucose. Metabolism was stopped and non-phosphorylated FDG was removed by washing the slices in 3x600μl chilled glucose-free BBRS. Brain slices were stored in 4% formalin in Dulbecco's phosphate buffered saline at 5^{0}C for at least 3 days.

2.2 Specimen preparation and production of planar surfaces

Over the course of 5 days, and subsequent washing to remove formalin, tissue slices were dehydrated in a series of increasing acetone (in %: 30x4, 50x4 70x5 90x5 and 100x5, 20 min each), followed by epon infiltration (acetone:epon by volume: 3:1, 1:1, 1:3 and 0:3). Epon was prepared for maximum hardness to minimize radiation damage [**4**]. Brain slices were reoriented in 100% epon and epon polymerization was performed at 70^{0}C for 2 days. Tissue blocks were shaped and then sectioned to a thickness of 3 μm on a conventional ultra-microtome, removing undesirable topographical information at the sample surface [4] and to enable scanning transmission x-ray imaging of the specimen in parallel with LEXRF detection.

2.3 LEXRF set-up and analysis

LEXRF measurements were performed at 909 eV with a 1 μm diameter X-ray microprobe, delivered by a Fresnel zone plate, providing an increase in the incident photon flux (10^{11} ph/s) by 10-fold compared to an earlier study [**4**]. A significant undertaking of the beamline upgrade was the doubling of silicon drift detectors (SDDs) from 4 to 8 SDDs in an annular configuration. Because X-ray fluorescence is isotropic, the number of detected fluorescence photons is proportional to the number of SDD's, thus enabling a reduction in dwell times from 50s to 10s per 1μm x 1μm pixel. The Kα emissions of O, N and F were monitored and expressed in LEXRF maps as the number of fluorescent photons collected per pixel without beam correction since the synchrotron current was maintained constant in top-up mode, a significant improvement from working in decay mode used earlier [**4**]. The LEXRF set-up was coupled to STXM imaging in both absorption and phase-contrast modes. Deconvolution of the

fluorescence spectrum per pixel was performed using the PyMCA Hypermet algorithm [**5**] and constant baseline subtraction.

3. Results

Subsequent to the upgrade of the Twinmic beamline and further optimization of ^{19}F detection, we aimed to explore the potential of LEXRF to image the stable isotope of fluorine in phosphorylated FDG (^{19}FDG-6P) at 1 μm^2 spatial resolution from brain structures closely resembling the general cerebral cytoarchitecture.

3.1 Metabolic and structural mapping of hypothalamic neurons

The ventral medial hypothalamus (VMH), a putative glucose sensing region of the brain, was chosen for illustrative purposes because of the large size of neurons and their dense clustering *in situ*, 4 of which are visible in Figure 1a. To differentiate structures, differences in the refractive index of biological matter (Fig. 1a) and LEXRF mapping of nitrogen (likely reflecting protein content) (Fig. 1b) were exploited. Nitrogen displayed high specificity for the neuropil (N), and 2 intracellular compartments in neurons: cytoplasm (*) and putative endoplasmic reticulum (ER, open arrows). As shown in Fig. 1c, ^{19}F in ^{19}FDG-6P was disproportionately high in the neuropil, punctuated by "hotspots" (closed arrows), reminiscent of dendritic swellings. A remarkable finding was the unequivocal localization of trapped ^{19}FDG-6P in the two aforementioned intracellular compartments of the cell body, best rendered when N and F maps were merged (Fig. 1d). Merging both Z elemental maps, moreover, unambiguously revealed two additional neuron cell bodies (outlined in yellow) -- not discernible by x-ray transmission imaging -- which have been sectioned through different planes as judged by cell body diameter

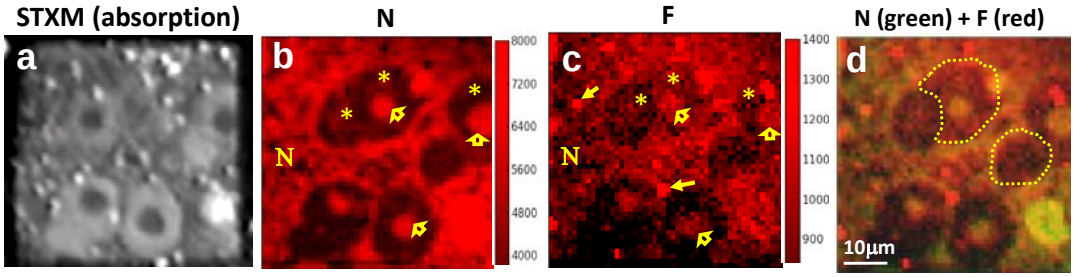

Fig. 1 Direct evidence of glucose metabolism by ventral medial hypothalamic neurons *in situ* and the use of endogenous nitrogen to map brain cytoarchitecture. Scale: photon counts.

and the presence or absence of putative ER. The distribution of ^{19}FDG-6P within the yellow outlines clearly illustrates the glycolytic capacity of these neurons (Fig. 1c). Together, such results, reproducible in 4 preparations, show that glucose metabolism occurs in VMH neurons and even moreso in the neuropil -- the region containing dendritic and axonal processes, synaptic connections, and glial endfeet processes.

3.2 Further structural mapping of hypothalamic neurons by LEXRF mapping of oxygen

In the example illustrated in Figure 2, LEXRF measurements were pursued within the ventral medial hypothalamus. Three neurons, identical to those shown in Fig. 1a, were readily identifiable in the absorption image (Fig. 2a, left hand side), while structures elsewhere were indiscernible. In striking contrast, the full-field structural content of the VMH of Fig. 2a was revealed in fine detail when the maps of oxygen (likely reflecting complex lipids) and nitrogen (likely reflecting protein content) were co-registered (Fig. 2b). Note the exquisite rendering of dendritic/axonal processes emanating from the cell bodies of 2 fusiform-shaped neurons located

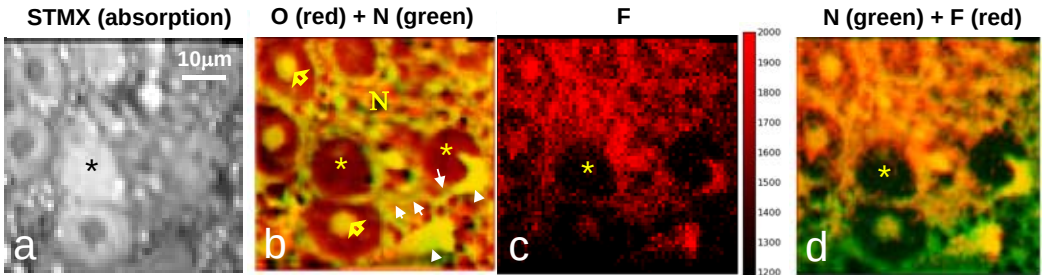

Fig. 2 Co-registration of O and N places glucose metabolism by 2 distinct neuronal cell types within a rich morphological and cytoarchitectural framework.

in the map at the lower right. The dendritic/axonal processes are indicated at the white arrows, while the white arrow heads point to the neuronal cell bodies. Co-registration of oxygen and nitrogen maps additionally delineated the neuropil (N) from the cell cytoplasm (*) and putative ER (open yellow arrows) of the large diameter neurons to a greater extent than seen in Fig. 1b, enabling the identification of 7 large diameter neurons sectioned through different planes of the cell body. This result exemplifies the inherent power of imaging multiple Z elements linked to endogenous organic molecules of the specimen to differentiate cellular structures used as landmarks. Like the neurons in Fig. 1c, the ^{19}FDG-6P distribution in large neurons situated in the upper half of Fig. 2c correlates well with nitrogen content (Fig. 2d). This relationship was modified in the microenvironment of the glycolytically active fusiform-shaped neurons.

4. Discussion

Imaging cerebral ^{18}FDG-6P in practice (Fig. 3) has been extended here to imaging ^{19}FDG-6P in one selected brain region with subcellular resolution. We exploited x-ray fluorescence imaging of F, O and N, where well-defined fluorescence cross-sections and the high brightness of the synchrotron source allowed obtaining element-specific information in the micron domain, showing that neurons from a functionally key region of the central nervous system resembling the general cerebral cytoarchitecture take up and phosphorylate glucose.

We first discuss the importance of LEXRF from the perspective of an ^{18}FDG PET neuroimaging scientist. We then discuss why LEXRF-based ^{19}F detection is extremely challenging, and how it might be extended even further. Finally, we discuss why LEXRF imaging of multiple Z elements potentially offers outstanding alternatives to conventional cell stains and dyes, and how the ^{19}FDG-6P results impact on current neuroscientific thought.

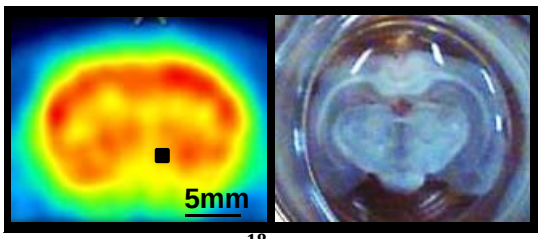

Fig. 3 Distribution of ^{18}FDG-6P in the coronal plane at Bregma -1.8mm of rat brain, placed next to the equivalent brain slice post-mortem.

Positron diffusion by virtue of ^{18}F decay limits the ultimate resolution attainable by PET and is the principle reason why the distribution of ^{18}FDG-6P (Fig. 3, at left) at steady-state appears as a blurry image of the rat brain (at right) at comparable stereotaxic brain coordinates. Given that the region of interest (black square) in the PET image covers the hypothalamus of the right hemisphere, non-invasive ^{18}FDG PET imaging allows, at best, quantitation of glucose metabolism from one brain region to another. Clearly, tackling the questions addressed in the Introduction requires micron resolution, unattainable with ^{18}FDG PET methodology. The commercial availability of non-radiolabeled FDG, i.e. ^{19}FDG, and the fact that the low Z

element fluorine is not endogenous to brain tissue per se -- subsequently confirmed experimentally, see Supplementary Data -- were together an attractive combination that led us to assess the application of synchrotron-based x-ray fluorescence to address cellular brain energy metabolism that underlies brain function.

Both methodologies are complimentary and synergistic, and each has its advantages and disadvantages, summarized in Figure 4.

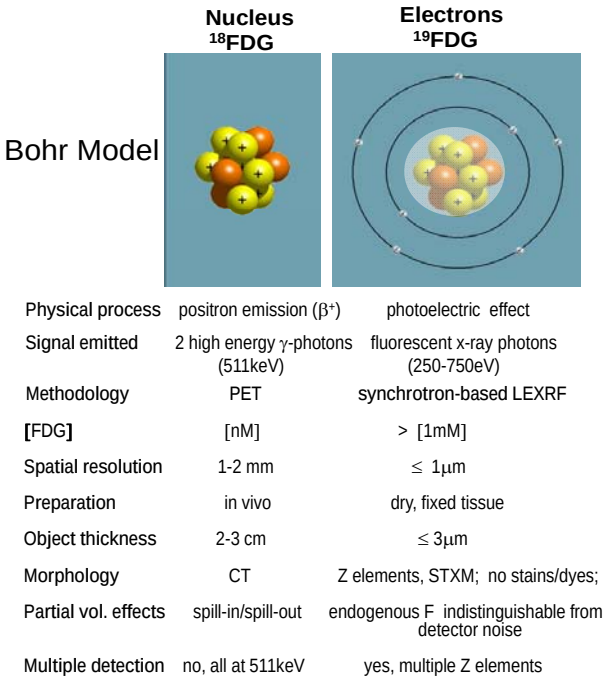

Physical process	positron emission (β^+)	photoelectric effect
Signal emitted	2 high energy γ-photons (511keV)	fluorescent x-ray photons (250-750eV)
Methodology	PET	synchrotron-based LEXRF
[FDG]	[nM]	> [1mM]
Spatial resolution	1-2 mm	≤ 1μm
Preparation	in vivo	dry, fixed tissue
Object thickness	2-3 cm	≤ 3μm
Morphology	CT	Z elements, STXM; no stains/dyes;
Partial vol. effects	spill-in/spill-out	endogenous F indistinguishable from detector noise
Multiple detection	no, all at 511keV	yes, multiple Z elements

Fig. 4 Salient features of ^{18}FDG positron emission tomography (PET) and synchrotron-based LEXRF of ^{19}F in ^{19}FDG-6P. In both methodologies F replaces the hydroxyl group at the second carbon of the glucose molecule. While the physical process is confined to the nucleus of the F atom in PET, that in LEXRF is confined to the electron orbitals of the F atom. To date, no other Z element conventionally linked to intracellularly trapped DG-6P, e.g. ^{3}H or ^{14}C [**4**] has the ability to be resolved as a stable element (at the second carbon) of the DG/DG-6P molecule from that linked to endogenous organic molecules comprising biological matter.

Three inter-related x-ray reasons and 3 metabolic-related reasons make LEXRF measurements of ^{19}F(DG-6P) extremely challenging. In the first case: (1) the low-energy incident photons needed to remove fluorine's core level electrons have low penetrating power; (2) F has inherently low fluorescence yields [**6**] due to low interaction cross-section, hence low probability of secondary photon emission; and (3) potential self-absorption in brain samples due to low energy, i.e, 676 eV fluorescence emission [**7**]. In the second case: (1) the transport of ^{19}FDG (at non-tracer amounts) into the cell was in direct competition with D-glucose, decreasing the amount of phosphorylated ^{19}FDG; (2) there is possible loss of DG-6P (^{19}FDG-6P), known to be soluble and diffusible during tissue fixation [**8**]; and (3) the distribution of trapped ^{19}FDG-6P cannot be a priori known as it depends on the distribution and affinity of glucose transporter proteins, brain region and stimulus conditions; and the level through which cells of the specimen were microtome-sectioned. The X-ray challenges have been largely overcome by the upgrade of the beamline and optimization of diffractive optics; challenges related to brain energy metabolism are multiple, and increasingly complex. Nonetheless, we are actively pursuing the metabolic experiments under physiological conditions in the live animal, and using a redesigned and high performance tissue fixation procedure.

Cellular brain nitrogen distribution displayed high specificity for the neuropil; and what we believe is the endoplasmic reticulum: currently the beamline set-up requires the removal of tissue water, mainly cytoplasmic, which was displaced by epon that is itself poor in N (see Supplementary data). Likewise, nucleoplasm, of similar low protein content as cytoplasm, was

also likely displaced by epon. Nevertheless, N and O mapping is structural, architectural mapping of nitrogen and oxygen linked to organic compounds found in living matter; their detection is independent of the dimensions of cellular and extracellular compartments—a serious impediment for the penetration of cell stains and dyes.

The high uptake of ^{19}FDG in the neuropil implies highly active glucose metabolism in astrocytes (glia cells) which individually occupy non-overlapping domains ~50 μm in diameter, to form a spatially patterned mosaic [**9**]. Given the low level of dendritic arborisation [**10**] and the importance of glutamate uptake into neighboring astrocytes [**11**], it is likely that glucose-metabolism is very high in active astrocytes occupying a large part of the cortical neuropil in an interwoven fashion. However, the expected distribution ^{19}FDG-6P in multiple cellular compartments, shown here for neurons, indicates that glial cells are not the exclusive site of glucose metabolism (and ^{18}FDG PET signal).

5. Conclusion

The present study describes the adaptation, optimization and use of synchrotron-based LEXRF imaging of fluorine in ^{19}FDG trapped as ^{19}FDG6P in biological tissue subsequent to the upgrade of the TwinMic LEXRF set-up to 8 SDDs. We conclude that LEXRF of F is a novel imaging approach that allows studying glucose metabolism at subcellular resolution *in situ*. We furthermore conclude that glucose metabolism occurs both in neurons and glial processes in brain structures resembling the general cerebral cytoarchitecture. Mapping endogenous N and O, in addition to transmission x-ray imaging, enabled placing F maps in a stunning morphological and cytoarchitectural context. Coupled to the subcellular resolution capabilities and the quantitative nature of elemental detection, synchrotron-based LEXRF and STXM together hold remarkable potential for assessing cerebral FDG metabolism. Extending this technology to high Z elements, i.e. Z > 50 and high-energy XRF on a suitable experimental x-ray beamline is expected to be more sensitive, as photon yield and penetration depths increase with Z [**12**].

Supported by the Integrated Infrastructure Initiative “European Light Sources Activities – Synchrotrons and Free Electron Lasers,” contract RII3-CT-2004-506008 (C. P-Y), the CIBM and Swiss National Science Foundation (131087, RG). We thank Professor Giorgio Margaritondo for the financial contribution to the purchase of 4 SDDs, and Dr Christian David at the PSI, Villigen, Switzerland for the Fresnel zone plate.

References

[1] Gianoncelli A, Kaulich B, Alberti R, Klatka T, Longoni A, De Marco A, Marcello A, and Kiskinova M 2009 Nucl Instr. Meth. Phys. Res. S **608** 195
[2] Frackowiak R S J, Magistretti P J, Shulman R G, Altman J S, and Adams M 2002 Strasbourg, Human Frontier Science Program Organization
[3] Cohen D M, Wei J, O'Brian Smith E, Gao X, Quast M J, and Sokoloff L 2002 Magn Reson Med **48** 1067
[4] Poitry-Yamate C, Gianoncelli A, Kaulich B, Kourousias G, Magill A W, Lepore M, Gajdosik V, and Gruetter R 2012 JNR (in press).
[5] Solé V A, Papillon E, Cotte M, Walter Ph, and Susini J 2007 Spectrochim Acta B **62** 63
[6] Hubbell J H, Trehan P N, Singh N, Chand B, Mehta D, Gard M L, Garg R R, Singh S and Puri S 1994 J Phys. Chem. Ref. Data **23** 339
[7] Hoefler H, Streli C, Wobrauschek P, Ovari M and Zaray Gy 2006 Spectrochimica Acta B **61** 1135
[8] Nehlig A, Wittendorp-Rechenmann E, and Lam C D 2004 JCBFM **24** 1004
[9] Halassa M, Fellin T, Takano H, Dong J-H, and Haydon P G 2007 J Neurosci. **27** 6473
[10] Mishchenko Y, Hu T, Spacek J, Mendenhall J, Harris K M, and Chklovskii D B 2010 Neuron **67** 1009
[11] Poitry-Yamate C, Vutskits L, and Rauen T 2002 J Neurochem **82** 987
[12] Paunesku T, Vogt S, Maser J, Lai B, and Woloschak G 2006 J Cell Biochem **99** 1489

Supplementary Data

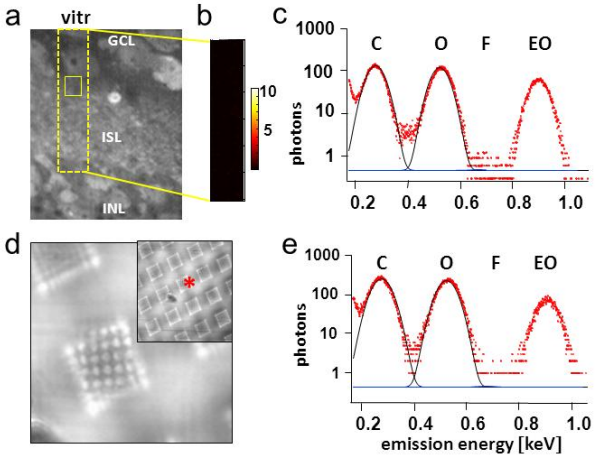

Supplementary Fig. 1 Fluorine is not endogenous to the specimen matrix nor to brain tissue. Modified from [4]. Inset: EM grid with epon matrix out of focus. * shows location of the LEXRF scan.

^{19}F mapped from the 3 innermost and glial-rich stratified layers of retinae (Suppl Fig. 1a), subsequent to exposure to 5mM D-glucose in place of ^{19}FDG, was absent (Suppl Fig. 1b), and normalized photon counts at 676 eV were indistinguishable from detector noise (Suppl Fig. 1c). Similar results were obtained from the specimen matrix, epon (Suppl Fig. 1d and e). Together, these results led us to conclude that the ^{19}F detected is derived from ^{19}F in ^{19}FDG. Since any non-phosphorylated ^{19}FDG was removed by washing [4] the fluorine detected was ^{19}F in ^{19}FG-6P.